Chall. Nano Micro Scale Sci. Tech., 9(1): 48-62, Winter and Spring 2021
DOI: 10.22111/CNMST.2021.36975.1202

ORIGINAL RESEARCH PAPER

Cancer Cell Separation Using Passive Mechanisms: a Review

Roya Mohammadali[1], Morteza Bayareh [1,*], Azam Usefian[2]

[1]Shahrekord University, Department of Mechanical Engineering, Shahrekord, Iran
[2]Department of Electrical Engineering, École de Technologie Supérieure (ÉTS), Canada

Received 23 December 2020; revised 11 September 2021; accepted 11 September 2021 available online 2 September 2021

ABSTRACT: The separation of micron-sized particles and their sorting is a critical issue in diagnosing cancer and biological analyses. For fast and accurate separation and sorting of circulating tumor cells (CTCs), various methods have been presented so far. CTCs which are responsible for cancer metastasis have the potential to provide significant prognostic and diagnostic values. In this paper, some procedures for the separation of CTCs are studied which are generally based on passive methods. These methods use the interaction between particles, flow field, and channel structure. In this study, various designs in connection with passive methods for separating and sorting CTCs are discussed, including filter/deformation, Pinched Flow Fractionation (PFF), Deterministic Lateral Displacement (DLD), inertia and Dean flow fractionation, tunable microfluidic systems, Hybrid microfluidics, and Carpet microfluidic chip technology. Overall, a list of challenges for the micro-fluidic-based cancer cell separation technologies needs to be dealt with to make them more applicable, useful, and ultimately more mature, from lab-oriented researches to real-world applications. It is suggested to perform numerical simulations by considering real shapes of rare cells. Besides, the impact of cell deformability, non-Newtonian impacts, and stretchable channels should be assessed in numerical examinations.

KEYWORDS: *Cell separation, CTCs, Passive method, Microfluidics*

INTRODUCTION

Cancer is regarded to be a leading cause of death all over the world, which accounts for 9.6 million deaths worldwide according to GLOBOCAN 2018 [1]. In other words, it has played an important role in terms of morbidity and mortality. Circulating tumor cells (CTCs) are the tumor cells that are shed from primary tumors and can travel to distant metastatic sites through circulation or even self-seed into their origin tumors. Although CTCs are rare in the blood (or lymphatic samples taken from cancer patients), they are widely thought to be a major cause of cancer deaths [2]. Indeed, they are an indication of cancer metastasis, disease progression, or survival [3]. To facilitate early cancer diagnosis, CTCs can be employed as biomarkers responsible for providing key bio-information of cancer tumor metastasis and deterioration. To do so, CTCs must be first detached from the primary tumor and then extravagated into the blood or lymphatic vessels [4-6]. The separation and sorting of cancer cells from untreated whole blood is an essential part of a variety of biological [7], biomedical [8], and clinical diagnosis applications [9]. The separation of particles is important for such applications as biomedical research and clinical diagnostics, which are typically performed by centrifugation, flow cytometry, gel electrophoresis, chromatography, etc.

*Corresponding Author Email: *m.bayareh@sku.ac.ir*
Tel.: +989131081858; Note. This manuscript was submitted on December 23, 2020; approved on September 11; published online September 2, 2021.

Based on differences in cellular biochemical properties (surface antigen expression), physical properties (size and deformability), or even in acoustic, magnetic, optic, or dielectrophoretic characteristics, a variety of technologies have been developed to separate CTCs from normal blood cells. Among various methods for CTC detection and enumeration, deformation-based CTC separation offers some advantages such as simple structure, stable performance, and also low cost. For example, orifice, weirs, ratchet, pillars, or membranes-based devices are from deformation-based CTC microfilters that can batch-process samples of whole blood without elaborating chemical labeling and provide a compelling label-free strategy for blood purification and cancer cell capturing. Since CTCs exist in the bloodstream of patients having cancer in a very low percentage and are the source of cancer metastasis [10, 11], CTCs separation technology has gained importance in recent years. Several methods have been presented for CTC separation which can be classified into two main categories as (i) passive and (ii) active methods. Passive separation methods employ the interaction between particles, micro-channel structure, and the flow field [12, 13].

Some of the most commonly used passive separation methods are inertial and dean flow fractionation, micro-hydro cyclone, and microfluidic separation methods [14] which will be discussed in the literature.

Passive microfluidic methods generally refer to the separation of cancer cells using their characteristics (density, size, channel structure, and surface antigen) and fluid flow properties, without considering external fields in microchips. Active methods use external actuators such as electric, magnetic, and acoustic fields to isolate microparticles or cells [15-17].

For instance, Shiriny and Bayareh [15] employed a Halbach array of magnets force to separate white blood cells (WBCs) and red blood cells (RBCs). The impact of the inlet Reynolds number and the distance between magnets and channels was evaluated to calculate the separation efficiency. Shiriny et al. [16] separated three sizes of polystyrene microparticles using a combination of inertial and magnetic forces. By changing the configuration of magnets, they determined their optimal situations in which 100% separation efficiency can be obtained. Passive separation methods have advantages over active ones. The most significant advantage is that they do not employ external fields for the separation process. In active sorting methods, on the other hand, the efficiency of particle sorting and throughput is relatively higher than passive ones. Therefore, passive separation methods are preferred for the applications in which the input energy is of critical concern, whereas active separation methods are applicable where higher efficiency in terms of particle sorting is required [18-19].

In this study, various designs in connection with passive methods for separating and sorting CTCs, including Filter/Deformation, Pinched Flow Fractionation (PFF), Deterministic Lateral Displacement (DLD), Inertia and Dean flow fractionation, Tunable Microfluidic Systems (TMS), Hybrid Microfluidics (HM), and Carpet Microfluidic Chip Technology (CMCT) are discussed.

PASSIVE MICROFLUIDIC-BASED CANCER CELL SEPARATION

Filter/Deformation

The device filtering process is simply based on the flow of sample blood cells passing through a filtering channel in a microfluidic chip. There is a critical pressure defined for each cell for squeezing through microfilter depending strongly on parameters like cell surface tension coefficient, cell diameter, and microfilter geometry. While the more deformable and smaller cells can simply pass the channel, the stiffer and larger ones are required to overcome large critical pressure. In addition, the latter will be blocked if there is not enough pressure provided. The deformation-based CTC separation method is a process for cancer detection by which CTC is trapped in cross-sectional geometries. One of the most significant steps in the design of deformability-based CTC separation devices is the design of microfilter geometries.

The pressure signature of a typical CTC deformation process was investigated for four different types of three-dimensional geometries, including circular, square, triangular, and rectangular, with uniform lengthwise cross-sectional areas [20]. Additionally, the CTC filter design was optimized. Figure 1 illustrates schematically the microfiltration setup. Carrier flow and CTC move from the left to the right along the microchannel.

Non-uniform reciprocal microfilters without locks were studied by Aghaamoo et al. [21], where different geometries, including conical-shaped and rectangular cross-section microfilters with different channel profiles, were selected as a case study. Three-dimensional and cut views of various geometries chosen for the CTC separation microfilter are shown in Figure 2. As can be seen, compared to rectangular-shaped microfilters, conical ones create a pressure signature nearly twice in range. According to the results, the two parabolic profiles lead to almost identical critical pressures that are higher than that of the corresponding linear profile. However, based on fundamental understandings of the cell separation process in filters, there is still a lack of design guidelines. To study conical-shaped microfilters, Aghaamoo et al. [22] performed numerical simulations, where deformability difference between CTCs and blood cells was employed for the separation process. In addition, pressure ratio was defined as a key parameter representing the ability to overcome clogging in such CTC separation devices and investigate the effect of conical angle on the optimum pressure ratio.

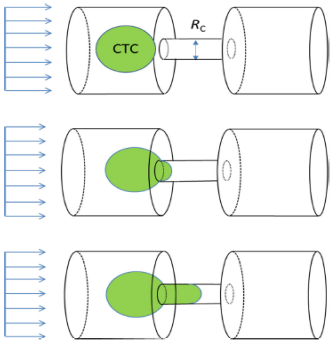


Fig. 1. CTC passing through a filtering channel [20].

Separation and measurement based on the size and deformation of CTCs obtained from patients suffering from resistant prostate cancer with re-adjustable traps were studied by Qin et al. [23], where the resettable cell trap was a two-layer PDMS structure comprising a sample-carrying upper flow channel and a lower fluid-filled control channel. The separation of these two layers was performed using a thin flexible diaphragm that could be inflated by applying an external pneumatic pressure to control the geometry of the two microchannels. According to the resettable cell trap, the surface of the flow channel was textured with two rows of micro-pockets and a center fin. To create an adjustable aperture capable of selectively trapping and releasing target cells, these microstructures

and the diaphragm were combined. Also, the position of the diaphragm could be considered to include two main states as (i) constricted state, where the diaphragm is in contact with the textured surface to reduce the aperture of the flow channel, and (ii) relaxed state, where the diaphragm is deflected away from the textured surface to enlarge the aperture of the flow channel.

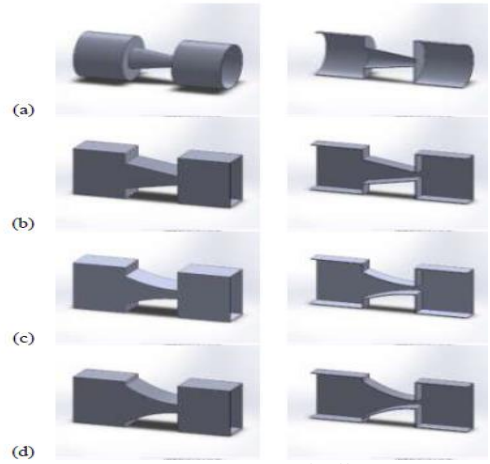


Fig. 2. 3D view and cut away view of different geometries selected for CTC separation microfilter: **a)** conical-shaped microfilter, **b)** rectangular-shaped with linear profile, **c)** rectangular-shaped with parabolic profile 1, and **d)** rectangular-shaped having parabolic profile 2 [21].

The filtration method applicable for size-based separation of microparticles was presented by Yoon et al. [24]. In microfluidic filtration systems, one of the most leading obstacles to having an efficient and continuous operation is the clogging of filters. To overcome the clogging of filters and allow continuous operation of filter-based microfluidic separation, a lateral flow microfluidic sieving (μ-sieving) technique was introduced. As a proof-of-concept of cancer cell separation, this technique was applied for separating fixed cancer cells from whole blood. The Schematic demonstrations of the μ-sieving principle are shown in Figure 3. To reduce the hydraulic pressure on the filtered tumor cells, the sample flow rate and the buffer flow rate were reduced to 0.2 ml/h and 0.1 ml/h, respectively. Under normal flow conditions, the shear rate at filters increases by trapping cancer cells as a result of raising thrombogenicity of whole blood as well as reducing fluid cross-section, which activates platelet. The coagulation of the hemocytes with the cancer cells led to complete blocking of filters preventing further operation.

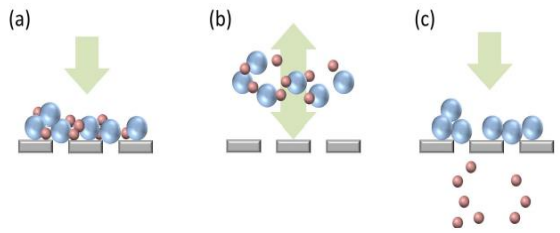


Fig. 3. Schematic demonstrations of the μ-sieving principle. **a)** Clogged filter during steady particles flow filtration, **b)** In-phase vibration of filtered particles with fluid oscillation, and **c)** Flowing of smaller non-target particles through the filter [24].

To avoid this type of coagulation, lysis of RBCs, centrifuge separation of RBCs, and anti-coagulant, or even both were performed in most filter-based whole blood CTC separation systems.

A novel microfluidic platform designed for marker independent capture of CTCs was introduced by Hvichia et al. [25]. The ParsortixTM cell separation system provided size and deformability-based enrichment with automated staining for cell identification in addition to subsequent recovery (harvesting) of cells from the device. By using the ParsortixTM system, the average cell capture inside the device had a range of 42% and 70%. Subsequent harvest of cells from the device also offered a range between 54% and 69% of cells captured. Most of all, 99% of isolated tumor cells were viable after processing in spiking experiments and also after harvesting from patient samples. Furthermore, as illustrated by mRNA characterization and array-based comparative genomic hybridization, these tumor cells were still applicable for the analysis of downstream molecular. Based on size and deformability, a procedure for the separation of CTCs from whole blood was presented by Park et al. [26] using the microfluidic ratchet device. To divert cells based on differences in size and deformability, this device leveraged the ratcheting motion of created single cells as they were deformed through funnel-shaped constrictions using oscillating flow. The principle of the microfluidic ratchet device relies on the asymmetrical force required to deform single cells through funnel-shaped constrictions. Figure 4 depicts the microfluidic ratchet mechanism. As shown, when the constriction opening is smaller than the diameter of the cells, the force required to push the cell through the constriction along the taper direction is less than that of the taper direction. Therefore, an oscillating flow of an appropriate magnitude produces a ratcheting transport based on a combination of cell size and deformability.

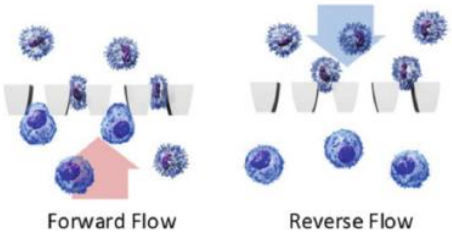


Fig. 4. Microfluidic ratchet mechanism [26].

A microfluidic construct for immunomagnetic separation of the particles of interest from the background cells was simulated by Shamloo et al. [27], where the separation unit was integrated with a mixer sub-unit. It was proven that the geometry of the device should be optimized before fabrication for condensing fixed assets. It was also shown that a thorough and detailed simulation will reduce the number of experiments in the subsequent step. By exploring particle trajectories, they optimized the outlet and magnets' positions. Some modifications were introduced on the primary geometry as well. First, an ancillary inlet channel was added to the geometry and, then, the increase in cross-section occurred gradually instead of using a prompt increase in the downward chamber. The mixer was envisioned for mixing the CTC enriched stream with lysis buffer to extract the biological material of the cell. Some modifications were provided on the mixing geometry, leading to the performance improvement of the functional unit. Among various devices, deformation-based CTC microchips have shown a strong promise for CTC detection. These devices involve a process by which CTCs are trapped while allowing more deformable blood cells to squeeze through the filtration geometry at the specified operating pressure. To design a reliable CTC microchip to enhance the performance of the device, in-depth perception of the cell passing process through the deformation-based microfluidic device is of great value. To describe cell scaling, the CTC pressure process was used through a microscopic filter channel with a non-Newtonian CTC model by Zhang et al. [28], where the pressure profiles at different flow rates were studied in a comprehensive investigation. Differences in terms of size and deformability between CTCs and blood cells, which would facilitate the development of technologies of size-based CTC isolation, were comprehensively summarized by Hao et al. [29]. Also, advances in microscopic technology for the early detection and detection of circulatory-related cancer in biomarkers were presented by Rana et al. [30], providing a comprehensive overview of all such microfluidic-based approaches for point-of-care cancer diagnostics, which offer some benefits like significantly reduced sample volumes with cost-effective and minimally invasive criteria.

Pinched Flow Fractionation (PFF)

PFF is a passive sorting technique that is applicable for the continuous sizing of particles in a microchannel utilizing the characteristics of laminar flow. PFF has been used for the separation of WBCs from LS174T colon cancer cells [31]. LS174T cells, as a convenient well-characterized colorectal cancer, have derived cell-line for modeling CTCs. This stems from the fact that the characteristics and size of LS174T cells are closely compatible with those of CTCs. Sketch of the PFF device fabricated by injection molding with five Luer fittings used as inlets and outlets is illustrated in Figure 5. As can be seen, particles are aligned and then sorted due to their size into different outlets. Particles having a diameter smaller than the critical diameter d_c flow towards the small particle outlet. İn the contrary, particles having a diameter larger than d_c flow towards the large particle outlet. The drain also collects most of the carrier solution. In addition, channel dimensions affecting the critical diameter are indicated. The four widths denoted width of (i) pinched segment W_p, (ii) small particle outlet channel W_s, (iii) large particle outlet channel W_l, and (iv) drain channel W_d.

In the PFF technique presented by Ref. [31], a sample containing particles of different sizes is placed in one inlet and a carrier solution is placed in the other inlet. The solutions from both inlets are then pushed into the device, where they meet at a narrow channel called the pinched segment. The particles then get aligned against the channel side-wall under the high flow from the carrier solution, and they follow streamlines according to the position of their center of mass. Downstream, the pinched segment is split into three outlet channels: (i) small particle outlet channel (ii) large particle outlet channel, and (iii) drain channel. Cells experience an increase in velocity as a result of the incoming fluid from the buffer inlet when moving from the sample inlet channel to the pinched segment. Simulations were used to investigate this elongation flow. It was also assumed that the cells travel at a height in the middle of the channel. Although the CTC recovery is independent of flow rates, the WBCs removal rapidly drops due to increased flow rates. A possible reason is that the inertia of the WBCs increases with the flow rates and eventually becomes large enough to deflect them from the streamlines going around the corner and into the small particle outlet. The throughput of a PFF device can be increased by increasing the depth. Here, the depth is limited by the maximum aspect ratio allowed by the Nickel electroplating step and the replication in polymer by injection molding.

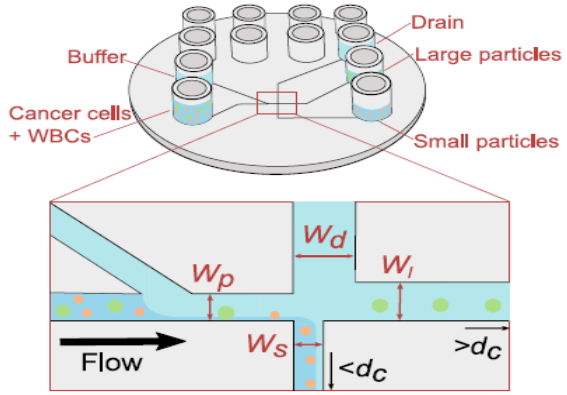


Fig. 5. Sketch of PFF device fabricated by injection molding with five Luer fittings used as inlets and outlets. (The four widths denote the width of pinched segment (W_p), small particle outlet channel (W_s), large particle outlet channel (W_l), and drain channel (W_d) [31].

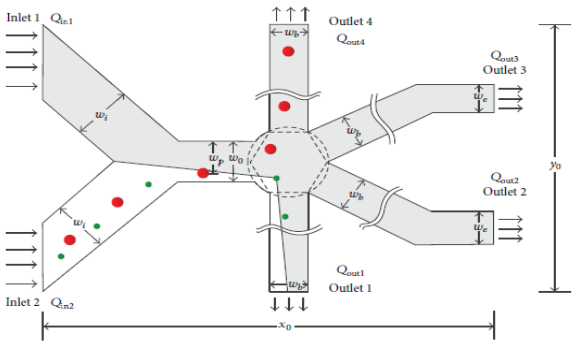


Fig. 6. The basic schematic structure of the simulated device proposed by Ma et al. [33].

The majority of current particle separation methods have only been demonstrated in Newtonian fluids. Experimental study of continuous particle separation in viscoelastic solutions via a combined action of elastic and inertial lift forces named elasto-inertial pinched flow fractionation (eiPFF) was provided by Lu et al. [32]. The parametric effects on eiPFF were systematically investigated in terms of dimensionless numbers. It was found that eiPFF offers much higher particle throughput and separation resolution than traditional steric effects-based PFF. Furthermore, particle separation via eiPFF does not monotonically increase with the elasticity number at higher polymer concentrations and is strongly influenced by the aspect ratio of channel width to its height. Numerical simulation of cell separation using simplified asymmetric pinched flow fractionation was examined by Ma et al. [33]. In the numerical model, which its basic schematic structure is indicated in Figure 6, the fluid motion was solved by the D2Q9 lattice Boltzmann model. The results demonstrated good agreement with the general results reported by other literature, showing the IB-LBM model accuracy. It was concluded that by regulating β (the outflow ratio at outlet 4), 8-μm and 16-μm cells can be sent into any one of all four D-branches.

Deterministic Lateral Displacement (DLD)

DLD microfluidic devices can provide a reliable label-free separation method for detecting CTCs in blood samples based on their biophysical properties. In DLD devices, most normal blood cells are expected to segregate into the small cell outlet. Blood is a heterogeneous mixture, so the size, shape, and deformability of blood cells are highly variable. Based on DLD theory, a periodic array of micro-posts shifted slightly along the fluid stream can be fabricated using Si substrate utilizing conventional photolithography and the Deep Reactive Ion Etching (DeepRIE) process [34]. To perceive the sorting behavior more easily, a narrow specimen streamline was formed by Okano et al. [35]. To do so, the specimen was supplied into a buffer flow from an inlet nozzle with a small volume ratio. As a result, although the throughput was not high enough, it was expected that there would be higher sorting efficiency and that channel clogging could be easily detected. The experimental setup includes the DLD chip and a glass cover, where approximately 109 cells were sorted with the DLD chip. As counting the whole specimen by FACS was impractical at the time of measurement, only a part of the sample was analyzed. To determine the portions of the analyzed specimen volume, recognized numbers of highly fluorescent beads (which can be distinguished from cells) were dispersed into the specimens collected after the sorting, and the beads were also counted simultaneously by FACS. Then, the separation ratio R was estimated as $R = C_L/(C_L+C_S)$, where C_L and C_S are the concentration of cells segregated into large and small cell outlets, respectively. It must be noted that a small number of cells were partitioned into the large cell outlet in all cases.

An effective design of the DLD microfluidic device for the CTC separation in the bloodstream was presented by Khodaee et al. [32], where a typical DLD array was designed and numerical simulations were performed to separate the CTC and WBCs (known as leukocytes) under various fluid flow conditions. The fluid-Solid Interaction (FSI) method was used to investigate the behavior of deformable cells in fluid flow. Furthermore, critical parameters affecting cell separation in the DLD microfluidic devices, including flow condition, cell deformability, and stress were investigated. Unlike leukocytes, the CTCs motion was independent of the flow condition and was laterally displaced even at higher Reynolds numbers. As larger CTCs cannot intercept the low-velocity fluid near the wall of the posts, they can

move faster and become separated from leukocytes. To reduce the cellular stress during the separation process, which results in increased cell viability and a more effective design of the microfluidic device, the results were used as a significant design parameter for the DLD fabrication [36]. DLD was used by Au et al. [37] to sort clusters through capitalizing on two geometric properties of size and asymmetry. Cultured breast cancer CTC clusters CTC(C)s containing between 2-100 + cells were recovered from whole blood using the integrated two-stage device with minimal cluster dissociation, 99% recovery of large clusters, cell viabilities over 87%, and greater than five-log depletion of red blood cells. The two-stage cluster capture operating principle is illustrated in Figure 7. The first stage of the microfluidic device "Stage 1" was designed to remove large clusters from whole blood using DLD, isolating large clusters based on their greater sizes. "Stage 1" consisted of an array of 50µm diameter, 90µm high poly dimethyl siloxane cylindrical micropillars with 63µm gaps between pillars, and row shift ratios of 1/7. To pass without clogging, these geometries were designed to deflect particles having 30µm or greater effective diameters while permitting very large clusters like those containing over 100 cells. While remaining clusters, cancer cells, and blood are shuttled into the inlet of the second stage "Stage 2", which was designed to sort clusters that failed to sort in "Stage 1" through discriminating asymmetric clusters from symmetric single cells.

Separating particles from 1µm to 10µm in one single DLD device is challenging because of the required diversity of pillar dimensions and inherent fabrication issues. An alternative method for obtaining E. coli bacteria from a blood sample with prostate cancer cells as provided by Pariset et al. [38], where cascading individual DLD devices were performed in a single automated platform by using flexible chambers. By doing so, the sample was collected and injected continuously between each DLD stage without any manipulation of the external sample. The authors presented a two-stage approach to automatically cascade several DLD purification steps in a single integrated platform. As a result of the modularity of the cascaded platform, any DLD chips can be implemented according to the application. Intermediate flexible chambers having high volume capacitance were directly integrated into the cartridge. They presented two advantages: (i) similar to single DLD devices, each DLD step was performed independently with optimized separation efficiency, and (ii) no external manipulation of the sample was required. It soul be mentioned that thanks to external actuation of valves and chambers controlling the sample flow between both DLD modules, each step of the purification protocol was performed automatically.

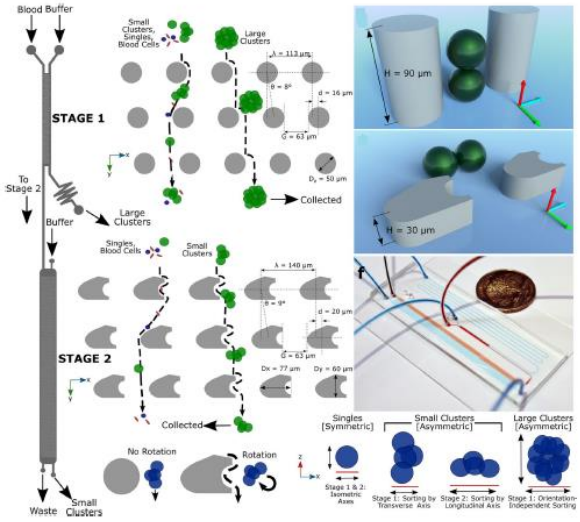


Fig. 6. Two-stage cluster capture operating principle [37].

An integrated microfluidic chip for efficient isolation and deformability analysis of CTCs was reported by Liu et al. [39], where the microfluidic chip integrated two modules: (i) one module was two mirrored DLD arrays for the depletion of blood cells and (ii) the other module was another DLD array with an increasing tilt angle for CTCs separation based on size and deformability. The chip allowed continuous isolation of CTCs with >90% capture yield as well as >50% capture purity at a throughput of 12 mLh^{-1}. Obtained results showed that the captured cancer cells maintained good viability. Downstream, deformability analysis validated that invasive MDA-MB-231 cells were more flexible than non-invasive MCF-7 cells. Notably, growing interest in utilizing high throughput DLD devices for practical applications like CTC separation necessitated employing higher flow rates in these devices, giving rise to operating in moderate to high Reynolds number regimes. Transport behavior of particles/cells was studied by Aghilinejad et al. [40] in realistic high-throughput DLD devices with hundreds of micro-posts through multiphysics modeling. Indeed, a practical formula was proposed for the prediction of the device's critical size, which could serve as a design guideline for high-throughput DLD devices. To predict the suspended particle's displacement, critical diameter (D_c) was defined in these devices, as it passed through the array of micro-posts. According to the geometrical parameters of the DLD post array shown in Figure 8a, any particle with a diameter less than the critical diameter ($D_p < D_c$) will follow a zigzag pattern without displacing laterally. On the other hand, a particle with a diameter greater than the critical diameter of the device ($D_p > D_c$) will cross streamlines and follow a bumped pattern, displacing laterally as it passes through the device. In other words, the array of micro-posts in DLD devices were in a specific arrangement that precisely controlled the trajectory of the

particle and facilitated the separation of particles larger/smaller than the critical diameter D_c. Furthermore, to study the post-cell interaction and evaluate its effect on cell motion behavior at moderate to high "Re" regime, three different post shapes shown in Figure 8b, including circle, triangle, and square were used for the DLD designs. As expected, a cell trajectory can be affected by the post shape.

Xiang et al. [41] reported a novel two-stage i-DLD sorter through coupling inertial microfluidics with DLD, offering precise, continuous, and size-based cell separation. While the first-stage spiral inertial microfluidic sorter was responsible for removing the vast majority of background blood cells in a high-throughput manner, the precise and flow-rate insensitive DLD sorter with triangular posts served as the second stage sorter, further removing the residual blood cells to obtain high purity tumor cells. Figure 9 depicts the working principle of the two-stage i-DLD device, coupling the spiral inertial microfluidic sorter with the DLD sorter for the precise, continuous, and label-free separation of rare tumor cells from background blood cells.

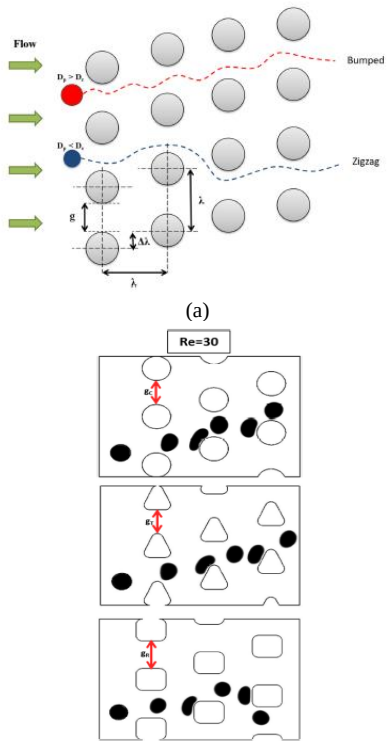


Fig.7. a) Geometrical parameters of DLD post array, **b)** Effect of post shape on cell trajectory at moderate to high Re regime [40].

Xiang et al. [41] introduced a microfluidic chip continuously isolating untouched CTC(C)s from large volumes of minimally (or undiluted) whole blood. Firstly, an array of 100µm-wide channels concentrated clusters in the blood, and then a similar array transferred them into a small volume of buffer. A microfluidic method for size sorting, a non-equilibrium inertial separation array (NISA), and 30 combining inertial focusing with repetitive flow-shifting were created. Size-based CTC and CTC(C) sorter built from enlarged non-equilibrium inertial separation arrays (NISA-XL) is presented in Figure 10. Compared to DLD, in which cells crossed streamlines when nudged by a post, NISA devices employed inertial lift to push cells away from channel walls in a size-dependent manner. Instead of small DLD posts and narrow channels, NISA devices incorporated longer rectangular islands, between which inertial focusing occurs in relatively wider channels.

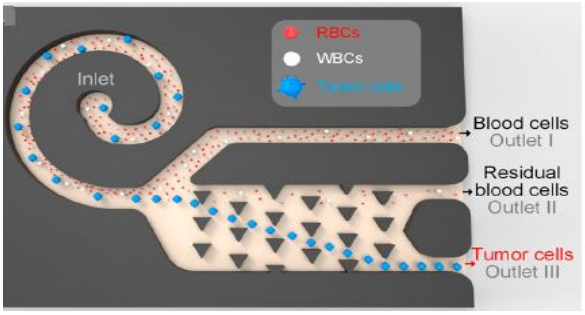


Fig. 9. The two-stage i-DLD device studied by Xiang et al. [41].

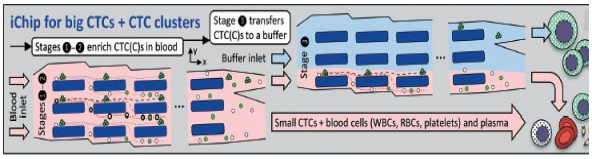


Fig. 10. Size-based CTC and CTC cluster CTC(C) sorter built from enlarged non-equilibrium inertial separation arrays (NISA-XL) [41].

Inertia and Dean Flow Fractionation

The integration of a micromixer unit for the creation of a cancer cell-microbead complex as well as an inertial flow unit for the detection and separation in a centrifugal platform was developed for the first time by Aguirre et al. [42], where the two units worked under different operational principles but both exploited the centrifugal pseudo-force. A high level of binding efficiency in addition to a mechanism for cell sorting and guiding with the established asymmetric inertial flow system was achieved by the units. The design of the passive micromixer took the advantage of centrifugal force in an orthogonal direction to create what has been termed ''flipping'' for increasing chaotic advection in the unit through turning the micro-channel contents 180º at each turn. To identify the maximum operational range, blood was spiked into the system. In non-spiked samples, cancer cells (MCF7) and microbeads bond together for generating cell-bead complexes (MCF7-PS) with a

binding efficiency of 97.1 %. However, blood-spiked samples of 2 % v/v blood content were found to have a separation of 92.5 %, which diminished further with increasing blood content (5 % v/v blood). Once the complexes entered the inertial flow unit under these conditions, they remained in high operational flow-focusing standard with up to 98.7 % ± 1.4 of the introduced cancer cells reaching the designated outlet. Notably, for both units, unpaired statistical "t" tests show P<5 with a 95 % confidence level. Aguirre et al. [38] integrated two units operating in flow-through mode. The two units operated continuously to maintain high-throughput processing of two solutions as (i) a solution with different percentages of blood-spiked with MCF7 cell numbers ranging from 1,050 to 250 and (ii) the 15-lm-diameter PS microbead solution. In addition to the mixing provided by Dean forces, the operational principle for this unit was the placement of the alternating sidewinding channels (see Figure 11), resulting in what they termed ''flipping'' to describe the behavior enhancing binding.

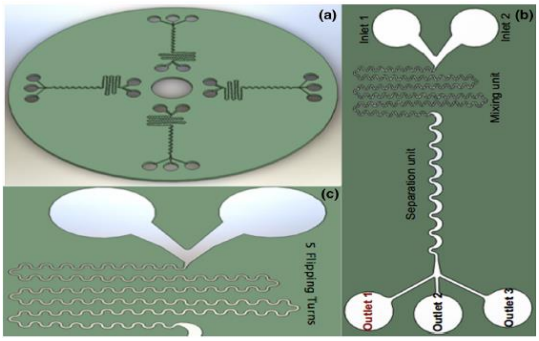


Fig. 11. a) Schematic of integrated lab-on-a-disc system, **b)** close-up of one of the four segments comprising disc, identifying the two inlets, mixing unit and the connected inertial flow-focusing channel, and **c)** zoom-in of mixing area depicting the five turns where flipping occurs in the integrated disc which enhanced mixing [42].

Sarioglu et al. [43] developed a microchip technology (the cluster-chip) to capture CTC clusters independently of tumor-specific markers from unprocessed blood. CTC(C)s were isolated through specialized bifurcating traps under low-shear stress conditions that preserve their integrity, and even two-cell clusters were captured efficiently. By using the cluster-chip, CTC(C)s were identified in 30-40% of patients with metastatic breast or prostate cancer or with melanoma. RNrnA sequencing of CTC(C)s confirmed their tumor origin and identified tissue-derived macrophages within the clusters. It is worth noting that efficient capture of CTC(C)s will enable the detailed characterization of their biological properties and role in metastasis. Pappas et al. [44] discussed recent advances in tumor cell culture, cancer cell analysis, and advanced studies enabled by microfluidic systems. Despite significant strides made toward CTC isolation, the separation of CTCs with high purity and high efficiency remains elusive. CTC separation is primarily limited by two factors. First, the separations are either size-based, which cannot offer a high degree of discrimination, or employ EpCAM antibodies to isolate cells. EpCAM antibodies in turn do not capture all cancer cell types and often require secondary identification like cytokeratin. The second obstacle in CTC separation is the low concentration of CTCs in most samples. Ebrahimi et al. [41] provided a detailed procedure of producing and using a label-free spiral microfluidic device to enable size-based isolation of viable CTCs utilizing hydrodynamic forces present in the curvilinear micro-channels. The procedure, which its general overview is presented in Figure 12, takes the advantage of distinct focusing positions of larger CTCs apart from smaller blood cells following combined inertial and dean drag forces in a spiral microfluidic device, which in turn enables rapid and continuous isolation of viable CTCs.

The simple geometry of Vortex HT shown in Figure 13 consists only of straight micro-channels and rectangular trapping regions, enabling straightforward device fabrication and sample processing procedures [46]. Vortex technology is a 70µm-depth polydimethylsiloxane (PDMS) device with an array of 40µm width straight channels, each leading to a series of 500µm×720µm rectangular trapping reservoirs, spaced 1000µm apart. At a high flow rate, large cells experience large inertial shear gradient lift forces, migrate across streamlines, and become stably trapped in laminar fluid micro vortices that develop in the reservoirs. Relatively smaller blood cells, however, do not experience a sufficient lift force to be stably trapped and may be washed away in a solution exchange that maintains cancer cell entrapment in vortices.

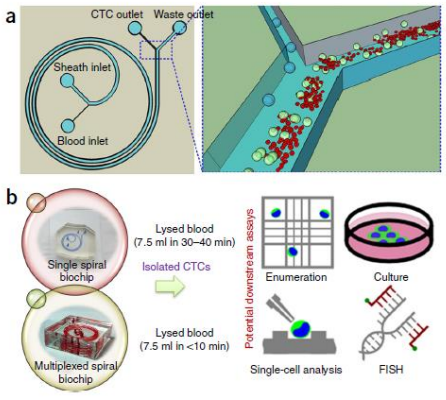


Fig. 11. General overview of CTC isolation using spiral microfluidics. **a)** Schematic of CTC enrichment by a spiral channel. **b)** Left-side: the optical image of single and multiplexed spiral biochips for high-throughput CTC isolation from lysed blood. Right-side: schematic illustrating possible downstream techniques for functional characterization of CTCs isolated using a spiral biochip [45].

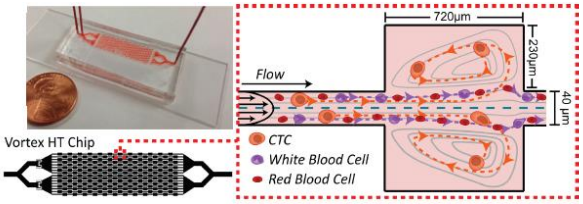


Fig. 13. The High Throughput Vortex Chip (Vortex HT) [46].

Ramachandraiah et al. [47] combined selective RBC lysis with focusing and separating nucleated cells based on differential inertial focusing in flow through spiral devices. The authors designed a spiral microchannel and optimized the flow and geometry parameters to focus and sort live cells. They proved that particles and cells flowing through curved spiral micro-channels experience two major forces as (i) lift forces (FL) caused by inertial flow and (ii) Dean forces (FD) resulting from Dean flow due to curvature. Depending on the relative magnitude of FL and FD acting on a particle, focusing close to the inner wall (dominant lift) or mixing (dominant Dean force) can occur. They focused on blood cell separation and conducted microspheres-based experiments and observations in ESI. Furthermore, according to the initial experiments, a 10-loop spiral channel device for blood cell experiments was designed. The impact of tank geometry on trapping cancer cell vortices was studied by Paiè et al. [48]. The effects of different reservoirs layouts on the efficiency of vortex-based devices, choosing geometries that facilitate the splitting of the trapped particles into two separate paths were investigated. To diminish the particle-particle interactions, these paths consist of the unchanged main vortex and a lateral circuit. Authors discovered that by properly choosing the lateral fluidic circuit dimension, it is possible to obtain a device capable of increasing the efficiency of vortex-based PDMS devices by 19%. To do so, the increased stability can be combined due to the larger reservoir area with the good trapping efficiency of the standard vortex chip. Khojah et al. [49] developed a passive capture method targeting a wide size range of cells through controlling flow conditions in single device geometry. This multimodal capture device was designed to generate laminar vortices in lateral cavities that branch from long rectangular channels. In this method, micro-vortices generated at lower Reynolds numbers could capture and stabilize large particles in equilibrium orbits or limit cycles near the vortex core. Other smaller particles or cells, on the other hand, could orbit near the vortex boundaries and be susceptible to exiting the cavity flow. Shen et al. [50] described an inertial microfluidic system containing a spiral microchannel for different highly efficient particle separations. Authors demonstrated that Dean-like secondary flow can be regulated utilizing geometric confinement in micro-channel. The inertial focusing arises from hydrodynamic forces acting on particles, which migrated laterally to equilibrium positions within the cross-section of the channel. It was widely recognized that the inertial lift forces were composed of the shear gradient lift force and the wall lift force. Configuration of the microfluidic device containing either dimension-confined spiral channel (left: D-channel) or normal spiral channel (right: N-channel) is depicted in Figure 14. As can be seen, the D-channel is equipped with ordered microstructures to change the flow field.

A Spiral microchannel with a stair-like cross-section for size-based particle separation was developed by Ghadami et al. [51], where a novel inertial separation method using spiral microchannel with stair-like cross-section was been studied. The authors investigated the fundamental design concepts as well as design criteria, and the effectiveness of the method has been examined by using a robust numerical model.

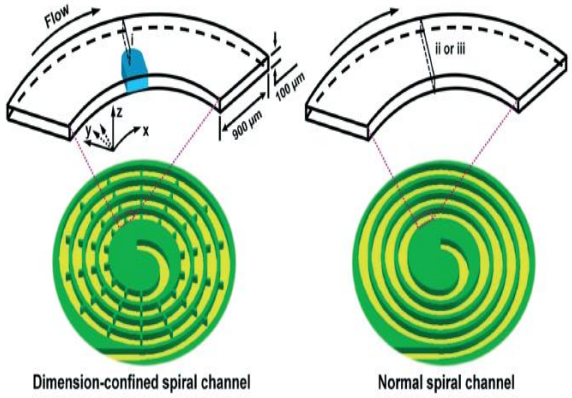


Fig. 14. Dean-like secondary flow acceleration induced by micro-bars in a spiral microchannel [50].

Moreover, the method was experimentally validated on a fabricated spiral microchannel. Based on the results, unlike conventional spiral microchannels, in which the flow vortices were located latitudinal, the two vortices are uniquely placed longitudinally in the stair-like cross-section. The basic design of conventional spiral microchannels and the proposed micro-channel are represented in Figure 15. It is worth noting that the geometry of the conventional spiral microchannel was inspired from the work done by Nivedita et al. [52], and the proposed spiral microchannel is designed by just varying the cross-sectional geometry of the conventional spiral micro-channel, while other design parameters are kept the same as the conventional design.

The design and operation of the fluid-assisted separation disc (FAST) disc were studied by Kim et al. [53], where the rationale used to design the FAST disc was that membranes having liquid-filled pores could provide a reduced pressure drop for size-selective filtration, resulting in gentler yet more efficient filtration. In the case of conventional filtration, the transport of liquid occurred

at a specific pressure that was higher than a critical value affected by interaction with solid surfaces, the pore size (geometry), and the surface tension. Abdulla et al. [54] introduced a cascaded microfluidic device consisting of two spiral channels and one zigzag channel designed with different fluid fields, including lift force, Dean drag force, and centrifugal force. Both RBCs-lysed human blood spiked with CTCs and 1:50 diluted human whole blood spiked with CTCs were tested on the presented chip. The chip simultaneously separated RBCs, WBCs, and two different types of tumor cells (human lung cancer cells (A549) as well as human breast cancer cells (MCF-7)) based on their physical properties. From the results, 80.75% of A549 and 73.75% of MCF-7 were faithfully separated from human whole blood. Furthermore, CTCs gathered from outlets could propagate and remain intact. The cell viability of A549 and MCF-7 were 95% and 98%, respectively. The separation of particles and cells in this chip relied on the dimensions and flow rates, which would affect the inertial lift force, Dean drag force, and centrifugal force. Flow rate simulation conducted by COMSOL is shown in Figure 15**.** It can be observed that the three-pointed position presents the same flow rate distribution inside the integrated channel as that in each counterpart.

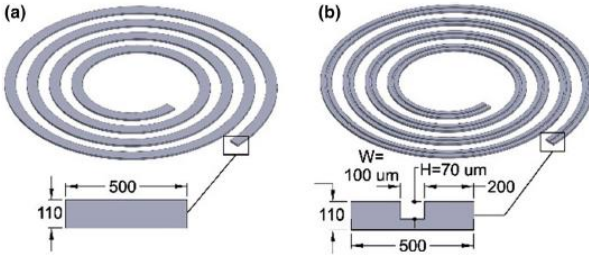


Fig. 14. a) Conventional spiral microchannel (Design 1), **b)** schematic of the proposed spiral microchannel with a stair-like cross-section (Design 2) [51].

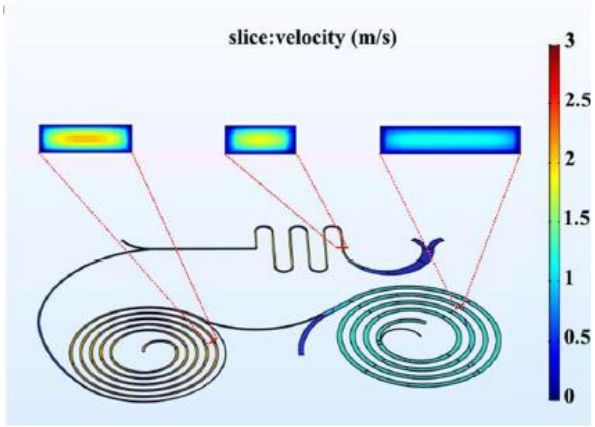
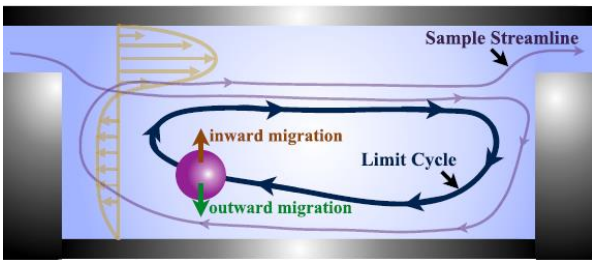


Fig. 15. Flow rate simulation conducted by COMSOL [50].

The separation of cancer cells using cyclic microcrystalline currents was studied by Haddadi et al. [55], where experiments were extended to address the engineering-physics of cancer cell entrapment in microfluidic cavities. First of all, the effects of channel width and device height on the morphology of the vortex were investigated. Then, the stable limit cycle orbits of finite-size cancer cells were presented. The authors demonstrated the effects of separatrix breakdown and limit cycle formation on the operation of the cancer cell separation platform. By studying the flow of dilute cell suspensions over the cavities, they further developed the notion of the cavity capacity and the relative rate of cell accumulation as optimization criteria connecting device geometry to the flow. Schematic of the continuous fluid exchange with the cavity and formation of a stable limit cycle trajectory for finite-size particles is illustrated in Figure 16. A novel multi-flow microfluidic device capable of sensitively providing high purity (>87%) of separation outcome without labeling was introduced by Zhou et al. [56]. The device was constructed and configured based on the phenomenal effect of size-dependent inertial migration. The separation microsystem was built upon the inertial migration of cells flowing in microchannels. Cells were subjected to inertial forces driving them toward equilibrium positions in two stages. In the first stage, cells migrated rapidly toward sidewalls of the micro-channel undergoing shear-induced lift force. Then in the second stage, cells slowly migrated to their equilibrium positions cantered on each sidewall under the influence of the rotation-induced lift force.



(c)

Fig. 16. Schematic of geometry studied by Hamed Haddadi et al. 2018 [55].

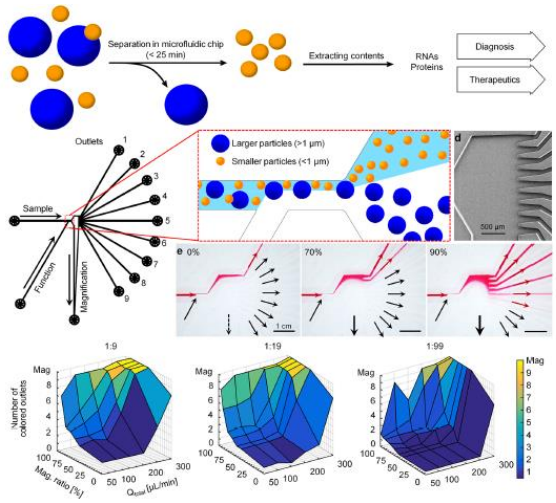
Tunable Microfluidic Systems

The complexity of a biological system can be resolved utilizing physicochemical properties to isolate and separate its specific constituent bio-organisms and molecules, such as cells, bacteria, proteins, and DNA [57]. Recently, there has been an emerging need to isolate and separate extracellular vesicles (EVs). EVs are lipid bilayer vesicles secreted by cells, and generally, their size ranges between hundreds of nanometers. Since EVs contain specific biomolecules like protein, mRNA, and microRNA, their potential application in diagnostics and therapeutics has garnered considerable attention. Shin et

al. [57] reported non-invasive size-based EV separation on a chip and analyzed separation patterns of micro-and nano-vesicles/particles. To perform EV separation based on heterogeneous sizes with diameters between 0.1 and 5μm, the authors used a microfluidic device whose design procedure and operational conditions are illustrated in Figure 17**.** Gwak et al. [58] reviewed the research trends in the isolation and analysis of CTCs using microfluidics. Microfluidics provides many attractive advantages for CTC studies, including continuous sample processing for reducing target cell loss as well as easy integration of various functions into a chip, making "do-everything-on-a-chip" possible. However, tumor cells obtained from different sites within a tumor exhibit heterogenetic features. Thus, heterogeneous CTC profiling should be conducted at a single-cell level after isolation to guide the optimal therapeutic path. The authors described the studies on single-CTC analysis based on microfluidic devices.

Hybrid Microfluidics

Antibody-free isolation and regulation of adherent cancer cells via hybrid branched microtube-sandwiched hydrodynamic system was studied by Feng et al. [59]. They demonstrated hybrid branched microtube arrays (HBMTA)-embedded hydrodynamic system that exhibited the capacity of antibody-free isolation of adherent tumor cells in addition to in situ regulation of the enriched tumor cells extracellular and intracellularly.



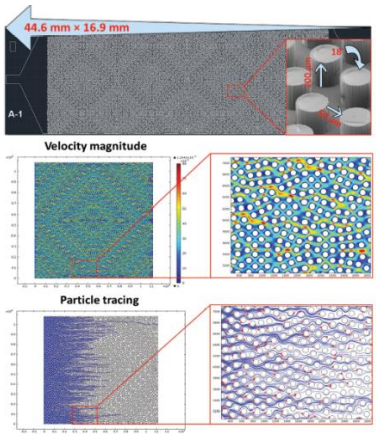
(c)

Fig. 17. Microfluidic chip design and operational conditions [57].

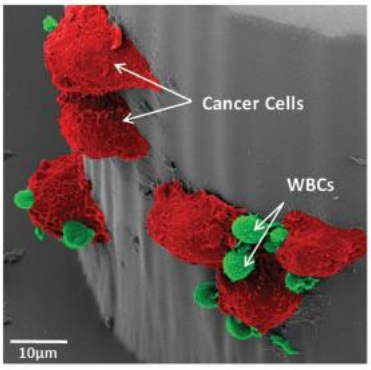
Carpet Microfluidic Chip Technology

The CTC Carpet Chip designed to capture heterogeneous populations of rare CTCs using antibody-coated micro-posts was modified by implementing an 18° rotation of hexagonal arrays of 100μm×100μm micro-posts with an average distance of 50μm between them. Novel re-arrangements of the posts were presented by Zeinali et al. [60], which greatly enhanced the capture of EpCs on one chip, while reducing off-target capture, including EMTCs. To do so, a dual immunoaffinity and physical discrimination approach enabled by using the lateral flow distribution and cell post interactions within the CTC Carpet Chip was employed. The CTC Carpet Chip had around 80000 micro-posts and the overall size of the microfluidic device was 44.6mm×16.9mm. The design of the CTC Carpet Chip and representative SEM images of the micro-posts are shown in Figures 18 a and b, respectively. To allow maximal contact between cells and micro-posts, the flow velocity was optimized, while shear forces were sufficient to prevent non-specific cell attachment to posts. In addition, different micro-post geometries and arrangements of the arrays and other parameters were explored in the process of optimization of the CTC Carpet Chip.

Table 1 summarizes the main characteristics of cancer cell separation performed using passive microdevices.



(a)



(b)

Fig. 4. a) Schematic representation of CTC Carpet Chip and finite element simulations, **b)** Pseudocolored SEM image of the captured cancer cells spiked into blood on the CTC Carpet Chip. Cancer cells and WBCs are shown in red and green respectively [60].

CONCLUSIONS

In this paper, an extensive review of various passive separation techniques is provided. Passive separation and sorting devices have a simpler structure and do not use external fields. The flow rate involved in passive

separation devices is relatively lower for which the process becomes relatively more time-consuming. The performance of these devices was characterized in terms of throughput and sorting efficiency. Due to the importance of cancer cell studies in the fields of biopharmaceuticals and clinical diagnosis, the effective separation of cancer cells or unwanted cell populations from cell mixtures has always been a popular focus of interest among researchers. Moreover, passive microfluidic methods capable of isolating different kinds of cancer cells have been discussed. Without an external field to drive cells, isolating different kinds of cancer cells involves a less complicated experimental setup. However, it often calls for fabricating a new device to address a new application. Overall, a list of challenges for the microfluidic-based cancer cell separation technologies needs to be dealt with to make them more applicable, useful, and ultimately more mature, from lab-oriented researches to real-world applications.

Table 1
Main characteristics of some passive microdevices that separate cancer cells.

Separation method	Cancer cell type	Sample	Ref.
Fishbone shape microchannel	Breast cancer	MCF-7 and a human erythrocyte mixture	[61]
Filtration	Microparticles	Blood	[62]
Inertial	MDA-MB-231, Jurket, K562, and Hela	Different mixtures	[63]
Micro-beads	CTCs	Blood	[64]
Hydraulic hump-based technique using micro-beads	Blood cells	Blood	[65]
Filtration	Rare cells	Surrounding cells	[66]
Herringbone channel	HL-60	Blood	[67]
Multistage hydrodynamic focusing	CTCs	Blood	[68]
Centrifugation	CTCs	Blood	[69]

REFERENCES

[1] Bray F, Ferlay J, Soerjomataram I, Siegel RL, Torre LA, Jemal A. Global cancer statistics 2018-GLOBOCAN estimates of incidence and mortality worldwide for 36 cancers in 185 countries. Cancer journal for clinicians (CA). 2018; 68(6): 394-424.

[2] Gupta GP, Massagué J. Cancer metastasis-building a framework. Cell. 2006; 127(4): 679-695.

[3] Plaks V, Koopman CD, Werb Z. Circulating tumor cells. Science. 2013; 341(6151): 1186-1188.

[4] Haddadi H, Naghsh-Nilchi H, Di Carlo D. Separation of cancer cells using vortical microfluidic flows. Biomicrofluidics. 2018; 12(1): 014112.

[5] Huang Q, Wang Y, Chen X, Wang Y, Li Z, Du S, Chen S. Nanotechnology-based strategies for early cancer diagnosis using circulating tumor cells as a liquid biopsy. Nanotheranostics. 2018; 2(1): 21.

[6] Tian F, Cai L, Chang J, Li S, Liu C, LinT, Sun J. Label-free isolation of rare tumor cells from untreated whole blood by interfacial viscoelastic microfluidics. Lab on a Chip. 2018; 18(22): 3436-3445.

[7] Chen CH, Cho SH, Tsai F, Erten A, Lo YH. Microfluidic cell sorter with integrated piezoelectric actuator. Biomedical micro devices. 2009; 11(6): 1223.

[8] Sackmann EK, Fulton AL, Beebe DJ. The present and future role of microfluidics in biomedical research. Nature. 2014; 507(7491): 181-189.

[9] Liu R, Chen X, Du Y, Yao W, Shen L, Wang C, Yuan Y. Serum microRNA expression profile as a biomarker in the diagnosis and prognosis of pancreatic cancer. Clinical chemistry. 2012; 58(3): 610-618.

[10] Shiriny A, Bayareh M. Inertial focusing of CTCs in a novel spiral microchannel. Chemical Engineering Science, 2020; 229: 116102.

[11] Lenshof A, Laurell T. Continuous separation of cells and particles in microfluidic systems. Chemical Society Reviews. 2010; 39(3): 1203-1217.

[12] Doddabasavana GB, PadmaPriya K, Nagabhushana K. A review of recent advances in separation and detection of whole blood components. World J. Sci. Technol. 2012; 2(5): 05-09.

[13] Kersaudy-Kerhoas M, Dhariwal R, Desmulliez MPY. Recent advances in microparticle continuous separation. IET nanobiotechnology. 2008; 2(1): 1-13.

[14] Lenshof A, Laurell T. Continuous separation of cells and particles in microfluidic systems. Chemical Society Reviews. 2010; 39(3): 1203-1217

[15] Shiriny A, Bayareh M. On magnetophoretic separation of blood cells using Halbach array of magnets. Meccanica, 2020; 55: 1903-1916.

[16] Shiriny A, Bayareh M, Ahmadi Nadooshan A. Combination of inertial focusing and

magnetoporetic separation in a novel microdevice. Korean Journal of Chemical Engineering, 2021; 38: 1686-1702.

[17] Ghorbani Kharaji Z, Bayareh M, Kalantar V. A review on acoustic field-driven micromixers, International Journal of Chemical Reactor Engineering. 2021; 19: 553-569.

[18] Bayareh M. An updated review on particle separation in passive microfluidic devices. Chemical Engineering and Processing-Process Intensification. 2020; 153: 107984.

[19] Sajeesh P, Sen AK. Particle separation and sorting in microfluidic devices: a review. Microfluidics and nanofluidics. 2014; 17(1): 1-52.

[20] Zhang Z, Chen X, Xu J. Entry effects of droplet in a micro confinement: Implications for deformation-based circulating tumor cell microfiltration. Biomicrofluidics. 2015; 9(2): 024108.

[21] Aghaamoo M, Xu J, ChenX. A Computational Study on Non-Uniform Cross-Sectional Deformability-Based CTC Separation Devices. ASME International Mechanical Engineering Congress and Exposition. American Society of Mechanical Engineers. 2015.

[22] Aghaamoo M, Zhang Z, Chen X, Xu J. Deformability-based circulating tumor cell separation with conical-shaped microfilters: Concept, optimization, and design criteria. Biomicrofluidics. 2015; 9(3): 034106.

[23] Qin X, Park S, Duffy SP, Matthews K, Ang BR, Todenhöfer T, Black PC. Size and deformability-based separation of circulating tumor cells from castrate resistant prostate cancer patients using resettable cell traps. Lab on a Chip. 2015; 15(10): 2278-2286.

[24] Yoon Y, Kim S, Lee J, Choi J, Kim RK, Lee SJ, OLee SB. Clogging-free microfluidics for continuous size-based separation of microparticles. Scientific reports. 2016; 6(1): 1-8.

[25] Hvichia GE, Parveen Z, Wagner C, Janning M, Quidde J, Stein A, Wikman H. A novel microfluidic platform for size and deformability-based separation and the subsequent molecular characterization of viable circulating tumor cells. International journal of cancer. 2016; 138(12): 2894-2904.

[26] Park ES, Duffy SP, Ma H. Microfluidic Separation of Circulating Tumor Cells Based on Size and Deformability. In Circulating Tumor Cells. Humana Press, New York, NY, 2017.

[27] Shamloo A, Ahmad S, Momeni M. Design and parameter study of integrated microfluidic platform for CTC isolation and enquiry. A numerical approach. Biosensors. 2018; 8(2): 56.

[28] Zhang X, Hashem MA, Chen X, Tan H. On passing a non-Newtonian circulating tumor cell (CTC) through a deformation-based microfluidic chip. Theoretical and Computational Fluid Dynamics. 2018; 32(6): 753-764.

[29] Hao SJ, Wan Y, Xia YQ, Zou X, Zheng SY. Size-based separation methods of circulating tumor cells. Advanced drug delivery reviews. 2018; 125: 3-20.

[30] Rana A, Zhang Y, Esfandiari L. Advancements in microfluidic technologies for isolation and early detection of circulating cancer-related biomarkers. Analyst. 2018; 143(13): 2971-2991.

[31] Podenphant M, Ashley N, Koprowska K, Mir KU, Zalkovskij M, Bilenberg B, Marie R. Separation of cancer cells from white blood cells by pinched flow fractionation. Lab on a Chip. 2015; 15(24): 4598-4606.

[32] Lu X, Xuan X. Continuous microfluidic particle separation via elasto-inertial pinched flow fractionation. Analytical chemistry. 2015; 87(12): 6389-6396.

[33] Ma JT, Xu YK, Tang XY. (2016): A Numerical Simulation of Cell Separation by Simplified Asymmetric Pinched Flow Fractionation. Computational and mathematical methods in medicine, 2016.

[34] Huang LR, Cox EC, Austin RH, Sturm JC. Continuous particle separation through deterministic lateral displacement. Science. 2004; 304(5673): 987-990.

[35] Okano H, Konishi T, Suzuki T, Suzuki T, Ariyasu S, Aoki S, Hayase M. Enrichment of circulating tumor cells in tumor-bearing mouse blood by a deterministic lateral displacement microfluidic device. Biomedical microdevices. 2015; 17(3): 59.

[36] Khodaee F, Movahed S, Fatouraee N, Daneshmand F. Numerical simulation of separation of circulating tumor cells from blood stream in deterministic lateral displacement (DLD) microfluidic channel. Journal of Mechanics. 2016; 32(4): 463-471.

[37] Au SH, Edd J, Stoddard AE, Wong AH, Fachin F, Maheswaran S, Toner M. Microfluidic isolation of circulating tumor cell clusters by size and asymmetry. Scientific reports. 2017; 7(1): 1-10.

[38] Pariset E, Parent C, Fouillet Y, François B, Verplanck N, Revol-Cavalier F, Agache V. Separation of biological particles in a modular platform of cascaded deterministic lateral displacement modules. Scientific reports. 2018; 8(1): 1-10.

[39] Liu Z, Chen R, Li Y, Liu J, Wang P, Xia X, Qin L. Integrated Microfluidic Chip for Efficient Isolation and Deformability Analysis of Circulating Tumor

Cells. Advanced Biosystems. 2018; 2(10): 1800200.
[40] Aghilinejad A, Aghaamoo M, Chen X. On the transport of particles/cells in high-throughput deterministic lateral displacement devices: Implications for circulating tumor cell separation. Biomicrofluidics. 2019; 13(3): 034112.
[41] Xiang N, Wang J, Li Q, Han Y, Huang D, Ni Z. Precise size-based cell separation via the coupling of inertial microfluidics and deterministic lateral displacement. Analytical chemistry. 2019; 91(15): 10328-10334.
[42] Aguirre GR, Efremov V, Kitsara M, Ducrée J. Integrated micromixer for incubation and separation of cancer cells on a centrifugal platform using inertial and dean forces. Microfluidics and Nanofluidics. 2015; 18(3): 513-526.
[43] Sarioglu AF, Aceto N, Kojic N, Donaldson MC, Zeinali M, Hamza B, Luo X. A microfluidic device for label-free, physical capture of circulating tumor cell clusters. Nature methods. 2015; 12(7): 685-691.
[44] Pappas D. Microfluidics and cancer analysis: cell separation, cell/tissue culture, cell mechanics, and integrated analysis systems. Analyst. 2016; 141(2): 525-535.
[45] Warkiani ME, Khoo BL, Wu L, Tay AKP, Bhagat AAS, Han J, Lim CT. Ultra-fast, label-free isolation of circulating tumor cells from blood using spiral microfluidics. Nature protocols. 2016; 11(1): 134-148.
[46] Che J, Yu V, Dhar V, Renier C, Matsumoto M, Heirich K, Pegram MD. Classification of large circulating tumor cells isolated with ultra-high throughput microfluidic Vortex technology. Oncotarget. 2016; 7(11): 12748.
[47] Ramachandraiah H, Svahn HA, Russom A. Inertial microfluidics combined with selective cell lysis for high throughput separation of nucleated cells from whole blood. Rsc. Advances. 2017; 7(47): 29505-29514.
[48] Paiè P, Che J, Di Carlo D. Effect of reservoir geometry on vortex trapping of cancer cells. Microfluidics and Nanofluidics. 2017; 21(6): 1-11.
[49] Khojah R, Stoutamore R, Di Carlo D. (2017): Size-tunable microvortex capture of rare cells. Lab on a Chip, 17(15): 2542-2549.
[50] Shen S, Tian C, Li T, Xu J, Chen SW, Tu Q, Wang J. Spiral micro-channel with ordered micro-obstacles for continuous and highly-efficient particle separation. Lab on a Chip. 2017; 17(21): 3578-3591.
[51] Ghadami S, Kowsari-Esfahan R, Saidi MS, Firoozbakhsh K. Spiral micro-channel with stair-like cross section for size-based particle separation. Microfluidics and Nanofluidics. 2017; 21(7): 115.
[52] Nivedita N, Papautsky I. Continuous separation of blood cells in spiral microfluidic devices. Biomicrofluidics. 2013; 7(5): 054101.
[53] Kim TH, Lim M, Park J, Oh JM, Kim H, Jeong H, Lee K. FAST: size-selective, clog-free isolation of rare cancer cells from whole blood at a liquid-liquid interface. Analytical chemistry. 2017; 89(2): 1155-1162.
[54] Abdulla A, Liu W, Gholamipour-Shirazi A, Sun J, Ding X. High-throughput isolation of circulating tumor cells using cascaded inertial focusing microfluidic channel. Analytical chemistry. 2018; 90(7): 4397-4405.
[55] Haddadi H, Naghsh-Nilchi H, Di Carlo D. Separation of cancer cells using vortical microfluidic flows. Biomicrofluidics. 2018; 12(1): 014112.
[56] Zhou J, Kulasinghe A, Bogseth A, O'Byrne K, Punyadeera C, Papautsky I. Isolation of circulating tumor cells in non-small-cell-lung-cancer patients using a multi-flow microfluidic channel. Microsystems & nanoengineering. 2019; 5(1): 1-12.
[57] Shin S, Han D, Park MC, Mun JY, Choi J, Chun H, Hong JW. Separation of extracellular nanovesicles and apoptotic bodies from cancer cell culture broth using tunable microfluidic systems. Scientific reports. 2017; 7(1): 1-8.
[58] Gwak H, Kim J, Kashefi-Kheyrabadi L, Kwak B, Hyun Ka, Jung HI. Progress in circulating tumor cell research using microfluidic devices. Micromachines. 2018; 9(7): 353.
[59] Feng J, Mo J, Zhang A, Liu D, Zhou L, Hang T, Yang J. Antibody-free isolation and regulation of adherent cancer cells via hybrid branched microtube-sandwiched hydrodynamic system. Nanoscale. 2020; 12(8): 5103-5113.
[60] Zeinali M, Murlidhar V, Fouladdel S, Shao S, Zhao L, Cameron H, Azizi E. Profiling heterogeneous circulating tumor cells (CTC) populations in pancreatic cancer using a serial microfluidic CTC carpet chip. Advanced Biosystems. 2018; 2(12): 1800228.
[61] Kwak B, Lee S, Lee J, Lee J, Cho J, Woo H, Heo YS. Hydrodynamic blood cell separation using fishbone shaped microchannel for circulating tumor cells enrichment. Sensors and Actuators B: Chemical. 2018; 261: 38–43.
[62] Lee YT, Dang C, Hong S, Yang AS, Su TL, Yang YC. Microfluidics with new multi-stage arc-unit structures for size-based cross-flow separation of microparticles. Microelectronic Engineering. 2019; 207: 37–49.
[63] Ozbey A, Karimzadehkhouei M, Kocaturk NM, Bilir SE, Kutlu O, Gozuacik D, Kosar A. Inertial focusing of cancer cell lines in curvilinear

microchannels. Micro and Nano Engineering. 2019; 2: 53–63.

[64] Sun N, Li X, Wang Z, Li Y, Pei R. High-purity capture of CTCs based on micro-beads enhanced isolation by size of epithelial tumor cells (ISET) method. Biosensors and Bioelectronics. 2018; 102, 157–163.

[65] Shirinkami H, Wang G, Park J, Ahn J, Choi Y, Chun H. Red blood cell and white blood cell separation using a lateral-dimension scalable microchip based on hydraulic jump and sedimentation. Sensors and Actuators B: Chemical. 2020; 307: 127412.

[66] Aljaghtham MS, Liu Z, Guo JJ, He J, Celik E. Numerical Simulations of Cell Flow and Trapping within Microfluidic Channels for Stiffness Based Cell Isolation. Journal of Biomechanics. 2019; 85: 43-49.

[67] Wickramaratne B, Ivey M, Pappas D. Isolation of proliferating cells from whole blood using Human Transferrin Receptor in a two-stage separation system. Talanta. 2019; 204: 731-738.

[68] Gao R, Cheng L, Wang S, Bi X, Wang X, Wang R, Yu L. Efficient separation of tumor cells from untreated whole blood using a novel multistage hydrodynamic focusing microfluidics. Talanta. 2019; 207: 120261.

[69] Bang D, Lee T, Park J, Lee G, Haam S, Park J. Enhancement of Capturing Efficacy for Circulating Tumor Cells by Centrifugation. BioChip Journal. 2018; 12(1): 38–45.